

Radiation Damage Study for PHENIX Silicon Stripixel Sensor

J. Asai^a, S. Batsouli^b, K. Boyle^c, V. Castillo^d, F. Douglas^e,
R. Ichimiya^a, Y. Inoue^f, M. Kawashima^f, T. Komatsubara^g, K. Kurita^f,
Z. Li^h, M. Nguyen^c, T. Murakamiⁱ, R. Nouicer^j, R. Pak^j, K. Sakashita^k,
K. Suga^f, A. Taketani^a, J. Tojo^a

^a *RIKEN (The Institute of Physical and Chemical Research), Wako, Saitama 351-0198, Japan*

^b *Oak Ridge National Laboratory, Oak Ridge, TN 37831, USA*

^c *Department of Physics and Astronomy, Stony Brook University, Stony Brook, NY 11794-3800, USA*

^d *Brookhaven National Laboratory, CAD Department, Upton, NY 11973-5000, USA*

^e *University of New Mexico, Albuquerque, NM 87131, USA*

^f *Rikkyo University, Toshima, Tokyo 171-8501, Japan*

^g *Institute of Physics and Tandem Accelerator Center, University of Tsukuba, Tsukuba, Ibaraki, 305-8577, Japan*

^h *Brookhaven National Laboratory, Instrumentation Division, Upton, NY 11973-5000, USA*

ⁱ *Department of Physics, Kyoto University, Kyoto, Kyoto, 606-8502, Japan*

^j *Brookhaven National Laboratory, Chemistry Department, Upton, NY 11973-5000, USA*

^k *Tokyo Institute of Technology, Meguro, Tokyo 152-8551, Japan*

Abstract

Silicon stripixel sensors which were developed at BNL will be installed for the RHIC-PHENIX silicon vertex tracker (VTX) in 2009. RHIC provides up to $2 \times 10^{32} \text{ cm}^{-2} \text{ s}^{-1}$ luminosity and the silicon stripixel sensors which are placed at 10 cm away from the colliding beams will suffer significant radiation damage. The effect mainly shows up as increased leakage current. It degrades a signal to noise ratio and may saturate the readout electronics.

We studied the radiation damage based on the RD48 result. The same diode which was made for RD48 study was used to our study and we call it reference diode. First we describe our reference diode irradiation test results which reproduced the relation between the irradiation fluence and the increase of leakage current of RD48.

Then we describe the beam experiments with stripixel sensor. The fluence of irradiated stripixel sensor was evaluated by the reference diodes by using 14.1 MeV neutron beam. We found its leakage current increase in the same way as that of the reference diode. And we experimentally irradiated to it at the PHENIX interaction region during the 2006 run. We showed the relation between the integrated luminosity and determined fluence from increase of leakage current. The expected fluence was up to Φ_{eq} (1 MeV neutron equivalent) = $3.1 \times 10^{12} \text{ Neq/cm}^2$ in RHIC operation for ten years. Finally we irradiated the expected fluence by using the 16 MeV proton beam.

Then we measured the increase of leakage current of irradiated stripixel sensor , it was Φ_{eq} (1 MeV neutron equivalent) = 2.5×10^{12} N_{eq}/cm^2 and $\Delta I = 7.4 \times 10^{-8}$ A/strip at 20 °C. And we estimated the operation temperature in PHENIX; $T \approx 0$ °C.

Key words: silicon, stripixel, radiation damage, VTX, RHIC, PHNIX

1. Introduction

We plan to build a silicon vertex tracker (VTX) and install it in the PHENIX detector in 2009. The VTX can identify heavy flavor quarks by the precise measurement of the decay vertex. It has a large solid angle which covers the acceptance of central arms. The jets from high energy quarks are measured by the central arms. The VTX has a barrel shape which consists of two inner layers of silicon pixel detectors and two outer layers of silicon strip detectors. For the inner two layers, we chose the ALICE pixels.(?) For the outer two layers, we chose a novel “stripixel” sensor which was developed by BNL and RIKEN. The detectors and electronics will be harshly irradiated in the PHENIX. The VTX operation has to be guaranteed for 10 years in RHIC running.

The preamplifiers are DC-coupled to each strips The preamplifier is known to saturate at 15 nA/strip in RHIC environment. Therefore, it is necessary to evaluate the leakage current accurately after a long term irradiation, typically for ten years of high luminosity RHIC operation.

CERN RD48 experiment has shown a good proportionality between irradiation fluence and increase of leakage current. The leakage current per channel is bigger for the stripixel sensor in the outer layers since the number of channels is smaller than that of the pixel sensor by two orders of magnitudes. Thus the stripixel sensors in the third layer which will be placed at 10 cm from a beam line is under the severest condition.

2. Silicon stripixel sensor

The two outer layers at the silicon vertex detector are composed of 246 stripixel sensors. The radial distances of the barrel shaped layers from the colliding beam are 10 cm and 14 cm. The high luminosity of RHIC, $2 \times 10^{32} \text{ cm}^{-2} \text{ s}^{-1}$, causes more radiation damage to stripixel sensor placed at 10 cm than 14 cm.

The silicon stripixel sensor was developed by BNL Instrumentation Division and RIKEN. It has two-dimensional single-side-readout strips. Two-dimensional readout is realized by charge sharing at each strip crossings when the radiation passes in a silicon. The concept is based on interleaved pixel electrodes arranged in projective X and U stereoscopic readouts. The stereo angle is about 4.6° . It allows compact arrangement without connecting electronics in the back. In 2005, mask design and processing technology, have been transferred successfully from BNL to the detector fabrication industry, the Hamamatsu Photonics, Japan (HPK), for mass production. The stripixel sensor specifications are summarized in Table 1. The layout is shown in Fig. 1. The readout side is implanted by p-type impurity and the back side is implanted by n-type impurity.

A stripixel sensor is wire-bonded to and readout by twelve SVX4 ASIC chips which have 128 channels each. A SVX4 ASIC which was developed by Fermi National Accelerator Laboratory and Berkeley National Laboratory collaboration is designed for the use with an AC-coupled device. But the stripixel sensor is a DC-coupled device. The advantage of the DC-couple is the higher S/N ratio. However, the SVX4 preampfire may be saturated by the leakage current of irradiated stripixel sensor. The preamplifier has

Email address: asai@riken.jp (J. Asai).

Table 1
Stripixel sensor property

Diode configuration	p+/n/n+
Resistivity	4-10 k Ω
Sensor size	3.43 x 6.36 [cm^2]
Sensitive area	3.072 x 3.000 x 2 [cm^2]
Thickness	625 [μm]
Pixel structure	Spiral structure 5 μm line, 3 μm gap
Effective pixel size	80 x 1000 [μm^2]
Strip construction	Chain of 30 pixels
Number of Strips	Total: 1536 X-strip: 384 x 2, U-strip: 384 x 2
Readout	DC couple
Front-end electronics	SVX4 ASIC

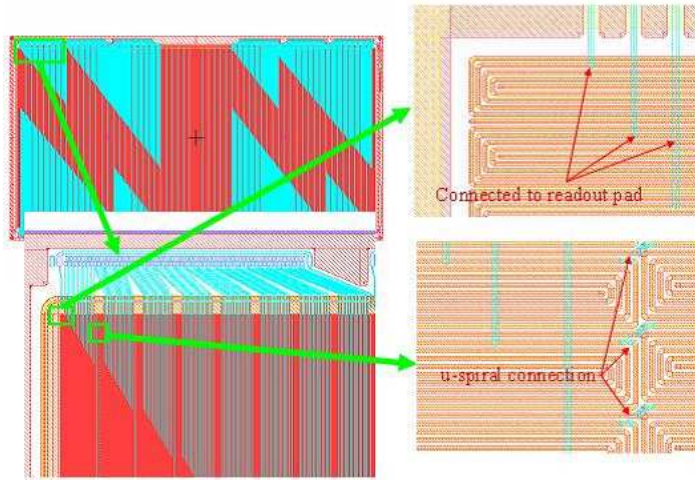


Fig. 1. Layout of the stripixel sensor by Hamamatsu Photonics

dynamic range of 200 fC and must be reset during a series of unfilled beam bunches which comes around every 13 μsec interval of the RHIC. Then it allows 15 nA/strip leakage current at maximum. The signal-to-noise ratio in the detector was found to be better than 20:1.

3. Radiation damage effect of silicon sensor

A silicon sensor suffers from radiation damage. There are three known radiation effects to the detector properties. They are (1) Increase of leakage current due to generation recombination of point defects. (2) Decrease of charge collection efficiency due to damage

induced trapping centers (3) Change of depletion voltage due to increase of effective acceptor point defects density.

The main effect which causes degradation in sensor performance is the increase of leakage current. It generates electric noise and may saturate the DC-coupled front-end electronics. We will write the problem/effect of (2) and (3). There are following relation in the increase of leakage current per volume $\Delta I/V$ and the fluence Φ_{eq} which is 1 MeV neutron equivalent fluence. The amount of leakage current increase depends on the type of radiation and the energy of their radiation. The factor which converts actual fluence to 1 MeV neutron equivalent fluence is known for large variety of types and large range of energy or the radiations; It is called hardness factor. CERN RD48 experiment has done an extensive study of the radiation damage on various silicon sensors for LHC.(?) The following useful equation was found by them,

$$\Delta I/V = \alpha \Phi_{eq} \quad (1)$$

Where α is the radiation damage parameter constant and depends on the thermal history from the start of the irradiation. The typical value is 4×10^{-17} A/cm after annealing for 80 minutes at 60 °C.

3.1. *IV/CV measurements*

The capacitance C decrease with increasing voltage V as:

$$C \propto 1/\sqrt{V} \quad (2)$$

It reach to full depletion. The voltage is called full depletion voltage V_{FD} . The determination of V_{FD} is used $1/C^2$ distributions depending on the bias voltage.

The leakage current I depends on the thickness of the depletion layer d and it increase with increasing voltage V as:

$$I \propto d \propto \sqrt{V} \quad (3)$$

The determination of ΔI between pre-irradiation and post-annealing is used at V_{FD} .

Leakage current depends on the temperature T [K] as:

$$I \propto T^2 \exp(-E_g/2k_B T) \quad (4)$$

Here, E_g is the energy gap of silicon ($E_g = 1.2$ eV); and k_B is the Boltzman constant ($k_B = 8.6 \times 10^{-5}$ eV/K). It holds for any Si sensors before and after irradiation. Therefore, the leakage current can be controled to some extent by adjusting the operation temperature. This relation will be used to evaluate the operation temperature for the SVX4 in RHIC II runs.

3.2. *Measurement system*

For the study of the silicon sensor property, we took two electrical measurements; capacitance and leakage current measurements as functions of the bias voltage. The circuit of measurement system is shown in Fig. 2. Bias voltage was supplied from the back of the stripixel sensor, and capacitance and leakage current were measured through readout pads. The measuring system consists of a picoammeter/voltage source (Keithley 6487), an LCR meter (HP 4263 B) and a switch scanner system (Keithley 7002). The

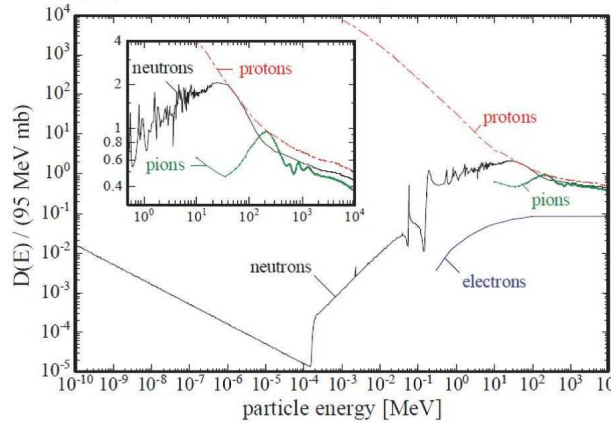


Fig. 3. Distribution of hardness factor

4.1. Confirmation the RD48 eference diode result

First we establish the radiation monitoring method of CERN-RD48 (ROSE) result. Their result showed proportions between the fluence and increase of leakage current with any particles in Fig. X. The fluence is defined as 1 MeV neutron equivalent. We used the diodes which were developed by CERN RD48 collaboration with the 12 MeV proton beam and 14.1 MeV neutron beam. The properties are shown in Table 7. For the electric measurement, the diode was wire bonded on the PCB board and connected to Lemo connectors which has bias line, ground line and readout line.

4.2. Beam monitors

We used a faraday cup and neutron counter for beam fluence monitor. A faraday cup is a detector by measured directly beam current of charged particle. It was worked in the magnet field for capture of scatterd electrons. The fluence was estimated from current integrator. It was used at 12 MeV proton beam experiment in Kyoto Unicersity.

A neutron counter was used at 14.1 MeV neutron beam test in Rikkyo University. The neutron counter was neutron dose rate meter: ALOKA TPS-451BS.

Table 2
RD48 diode property

Diode configuration	p ⁺ /n/n ⁺
Resistivity	2 [kΩ]
Active area	2.5×10 ⁻¹ [cm ²]
Thickness	3.04×10 ⁻² [cm]
Volume	7.6×10 ⁻³ [cm ³]

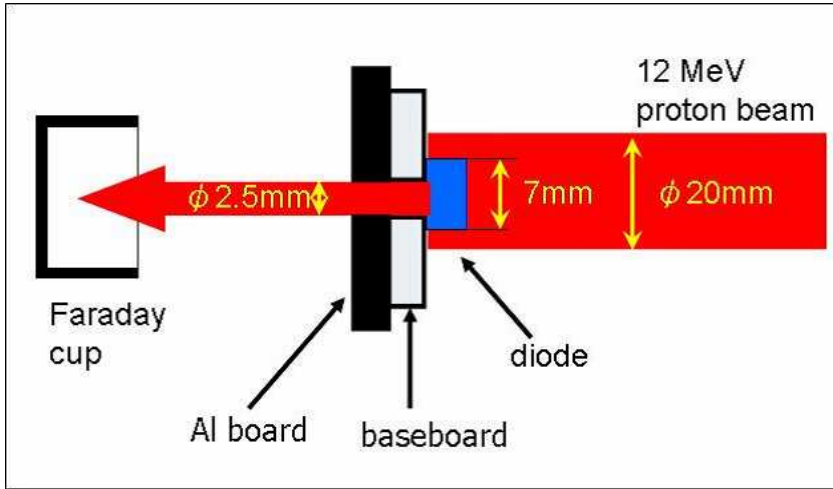


Fig. 4. Beam test setup with 12 MeV proton

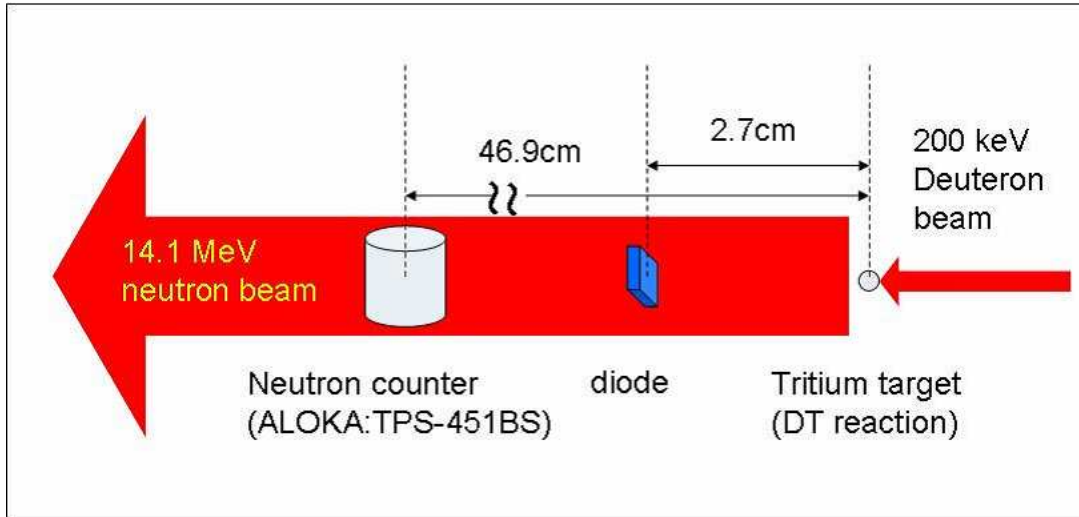


Fig. 5. Beam test setup with 14.1 MeV neutron

4.3. Beam test by reference diode

The RD48 diodes were irradiated for reproduction of radiation monitoring method. The leakage current and capacitance were measured before irradiation and after annealing. The annealing was done for 80 min at 60 °C.

We studied the irradiation test with four silicon diodes using 12 MeV proton beam from Tandem accelerator at Kyoto. The integrated fluences were 1×10^{11} , 1×10^{12} , 1×10^{13} [N_{eq}/cm^2]. We estimated the correspondence between beam monitor fluences and diode fluences. The beam fluence estimated with beam information of the faraday cup measurement and hardness factor. The hardness factor is depending on the particle and

the energy, and converts to the fluence of 1MeV neutron equivalent is estimated. The hardness factor of 12 MeV protons is 3.636 +- 0.112. The diode fluence estimated with increase of leakage current between pre-irradiation and after-annealing, and damage parameter α which is estimated using temperature history of thermochron data. The result distribution of comparison shows in Fig. 8. The confirmation is agreement within 25%.

We studied radiation fluence with the silicon diode using 14.1 MeV neutron beam from the Cockcroft-Walton accelerator at Rikkyo. The fluences were 1×10^{10} and 1×10^{11} [N_{eq}/cm^2]. The beam fluence estimated from faraday cup and the neutron counter. The hardness factor of 14 MeV neutron is 1.823 +- 0.006. The fluences of diodes were estimated by the same method as 12 MeV proton beam. The result distribution of comparison is in Fig. 8. The confirmation is agreement within 40%.

We confirmed the measuring method same as RD48 results to estimate the fluence of the silicon diodes using different particles and energy. Figure 8 shows the fluences which were two lower fluences of 14.1 MeV neutron beam test and four higher fluences of 12 MeV proton beam test. It was described the good agreement between the fluence from diode measurement and beam information. Next we studied the radiation damage of silicon stripixel sensor with the measuring method by the reference diode.

Table 3
Beam test result with reference diodes

Diode number	1	2	4	5	8	7
Beam particle	proton	proton	proton	proton	neutron	neutron
Beam energy [MeV]	12	12	12	12	14.1	14.1
$\Delta I/V$ [A/cm^3]	1.98×10^{-4}	2.73×10^{-4}	3.06×10^{-5}	5.08×10^{-4}	1.07×10^{-6}	2.66×10^{-6}
α [A/cm]	4.09×10^{-17}	4.12×10^{-17}	4.11×10^{-17}	4.19×10^{-17}	4.11×10^{-17}	4.05×10^{-17}
Diode fluence [N_{eq}/cm^2]	4.85×10^{12}	6.63×10^{12}	7.44×10^{11}	1.21×10^{13}	2.61×10^{10}	6.57×10^{10}
Proton beam pulse [$/\times 10^{-10} C$]	122	125	12	251	-	-
Total beam current [μAh]	-	-	-	-	28.8	126.8
Neutron beam count [$/cm^2$]	-	-	-	-	9.94×10^7	4.49×10^8
Z distance neutron counter [cm]	-	-	-	-	46.9	46.3
Z distance diode [cm]	-	-	-	-	2.71	4.41
Beam fluene [$/cm^2$]	1.55×10^{12}	1.59×10^{12}	1.53×10^{11}	3.20×10^{12}	2.98×10^{10}	4.96×10^{10}
Hardness factor κ	3.636	3.636	3.636	3.636	1.823	1.823
Beam fluene [N_{eq}/cm^2]	5.62×10^{12}	5.79×10^{12}	5.56×10^{11}	1.16×10^{13}	5.43×10^{10}	9.04×10^{10}

5. Test at PHENIX IR

One main concern for the vertex detector is the radiation it will be exposed to during the RHICII operations. In particular the maximum dark current that the SVX4s are allowed to see is 15 nAmp, which is determined by the speed that the preamplifiers can be reset. In order to better understand the radiation that the strip-pixel sensors will be exposed to during RHICII operations and the resultant possible damage, we performed

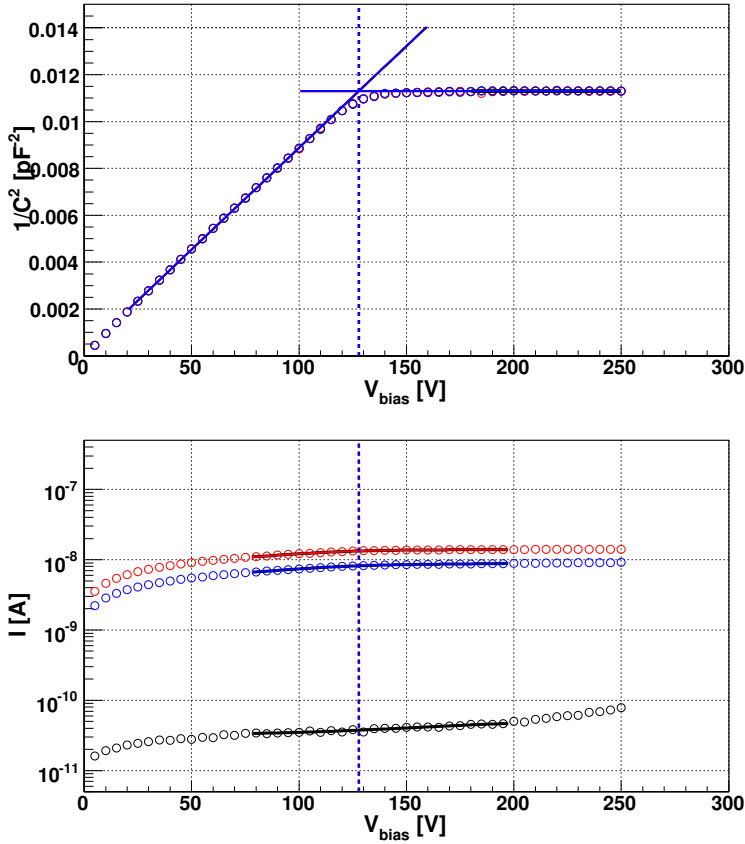


Fig. 6. IV/CV measurements result by reference diode8 with 14.1 MeV neutron beam

detailed measurement of the radiation dose in the PHENIX IR (Interaction Region) during the run6 pp run.

Three Beam Loss Monitors (BLMs), two chipmunks, sixteen pin diodes and thirty TLDs were installed at the PHENIX IR area, at various radii underneath the interaction point for the measurement of the instant and accumulated radiation dose during run6. Figure 9 shows the position of the Radiation measurement structure underneath the beam pipe in the IR area of PHENIX. Figure 10 shows the position of the BLMs and chipmunks in the Radiation measurement structure (in inches). The top strip of the structure is positioned 10cm away from the beam pipe. Two strip-pixel sensors were placed on the top stripe of the structure so as to measure the radiation damage during the run and two thermocouples, three thermochrons were positioned near the strip-pixels so as to keep track of the temperature during the irradiation period. Figures 11 and 12 are pictures of the structure and the top strip where the strip-pixels are positioned.

The Beam Loss Monitors are not sensitive enough to respond to the normal RHIC operation radiation in the current pp run. They could detect potential acute radiation. The chipmunks were used to measure instantaneous Luminosity and Radial dependence of the radiation. The TLDs to measure integrated dose and more extensive Radial depen-

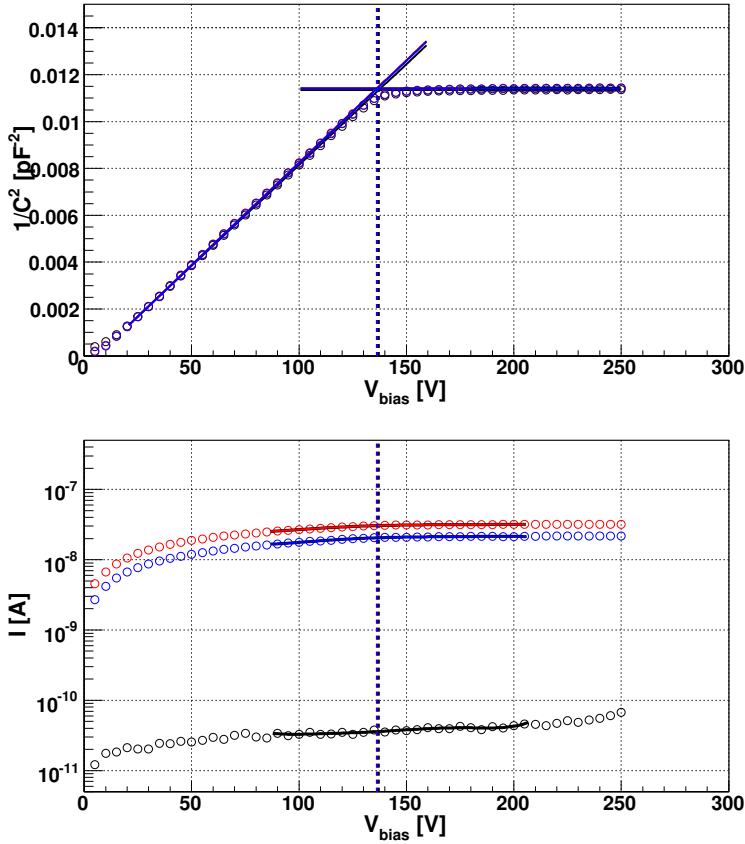


Fig. 7. IV/CV measurements result by reference diode7 with 14.1 MeV neutron beam

dence. Finally the strip-pixel and pin diodes were used to measure the actual effect in units we care about. The information from the chipmunks and the TLDs can then be used to get RHIC II scaling factors and thus scale accordingly the strip-pixel and pin diode current measurements.

5.1. Chipmunks

The Chipmunks (C-AD Personnel Radiation Monitoring Instruments) provide a sensitive way to monitor the instant radiation rate in the IR. The Chipmunks are configured to read in Dose Equivalent units, i.e. “mrem/hr” on a meter. There is also an accompanying frequency output (Hz) that is proportional to the meter reading, determined by the C-AD Personnel with the use of a Test Source Cs-137. It was determined that for chipmunk1 (positioned at 63cm distance from the beam pipe) $4.68 \text{ Hz} = 42 \text{ mrem/hr}$, and for chipmunk2 (positioned at 33cm distance from the beam pipe) $4.86 \text{ Hz} = 43 \text{ mrem/hr}$. In order to convert the Dose Equivalent measured by the chipmunks to Absorbed Dose in units of rad we have to use the following formula:

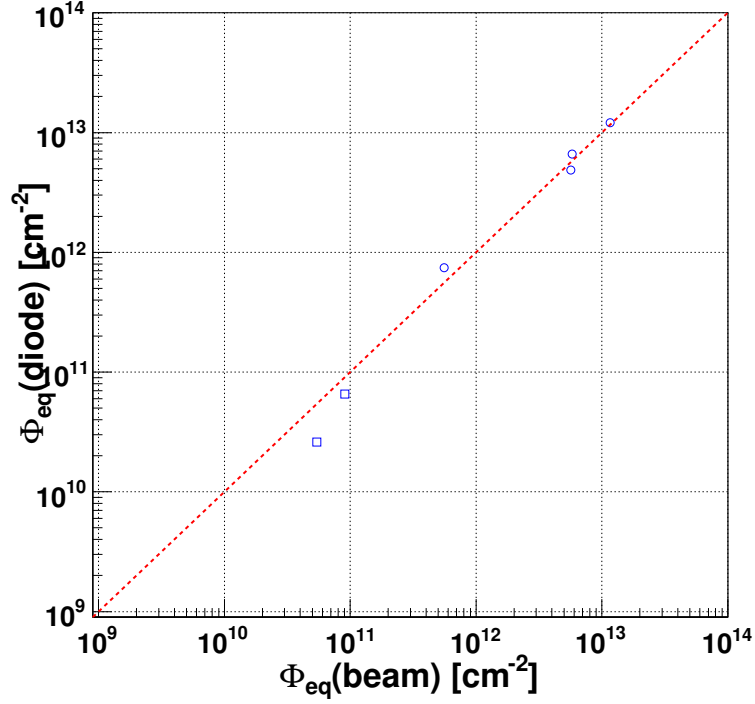


Fig. 8. Distribution of comparison fluence between diode and beam information

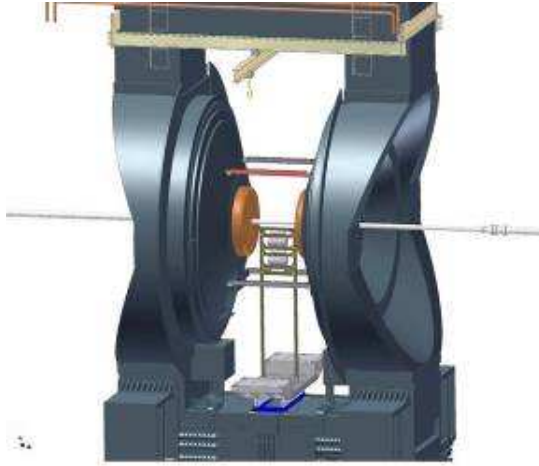


Fig. 9.

$$DoseEquivalent(rem) = AbsorbedDose(rad) * QualityFactor. \quad (9)$$

The Quality Factor term depends on the Radiation environment and should be determined specifically for the PHENIX environment. Instead, the currently used approximation for the Accelerator environment, Q.F =2.5, was used for PHENIX also. Thus,

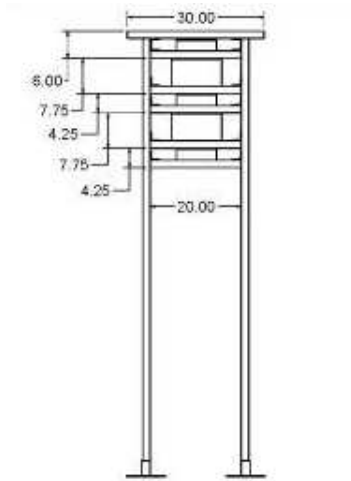


Fig. 10.



Fig. 11.

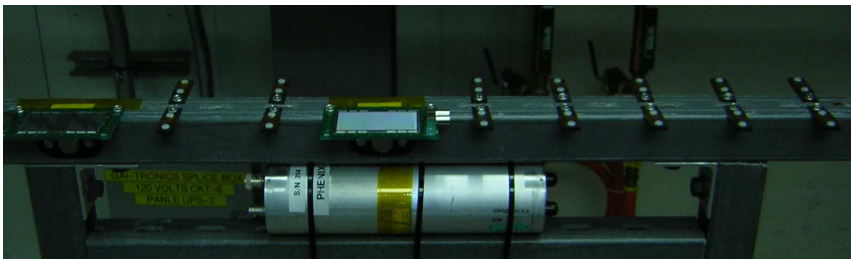


Fig. 12.

the overall conversion from the frequency output to Absorbed Dose were determined to be 1counts/sec = 1 microRad/sec for chipmunk1 (positioned at 63cm distance from the

beam pipe) and 1 counts/sec= 0.99 microRad/sec for chipmunk2 (positioned at 33cm distance from the beam pipe). We should note again that the Quality Factor used has not been specifically and accurately determined for the PHENIX environment. However for the purposes of the study, which is to identify radiation dose characteristics with respect to beam conditions and luminosity the absolute values are not so important.

As seen in figures 13 and 14 the chipmunk features (count/sec versus time) are very similar to the ZDCNS measurement for a typical RHIC store. The initial structure (from 04/08/06 15:30 to 04/08/06 15:47) corresponds to the ramping, steering of the beams in the blue/yellow rings and then the peak after time 15:47 to 16:00 corresponds to beam collisions having started but prior to the collimation of the beams. The spike in ZDC as well as the chipmunk corresponds to the two beams seeing each other and the ions in the periphery of the beam interacting with each other. Once the beams have been collimated the beam “halo” goes away so the radiation dose goes down.

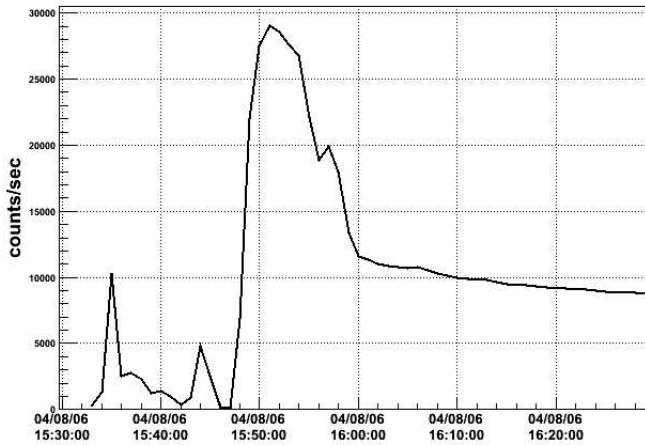


Fig. 13.

5.1.1. Dose dependence on Radial distance from the Interaction Point

The measurements from the two chipmunks can be used to quantify the radial dependence of the absorbed radiation. In Figure 15 the ratio

$$R_{radii} = \ln(C2_{Count}/C1_{Count})/\ln(R2/R1) \quad (10)$$

for a typical store is plotted, where $C2_{Count}$, $C1_{Count}$ are the measured rates converted in microRad/sec at chipmunk2 and chipmunk1 respectively and R2, R1 the distance of chipmunk2, chipmunk1 (R2=33cm, R1=63cm) from the beam pipe. The ratio for the post-collimation phase (figure 16) indicates an almost radial dependence ($1/r^{1.83}$) where r is the distance from the interaction point. An exact $1/r^2$ dependence would imply that the chipmunk sees a point like source from the interaction point. The reason for the deviation from $1/r^2$ could be that the radiation is more like a combination of a point source and a line source. On the other hand it could be an effect of the magnetic field. Low momentum particles could be trapped in the magnetic field and transverse the chipmunk canister multiple times, thus resulting in higher counts. For a zero field run

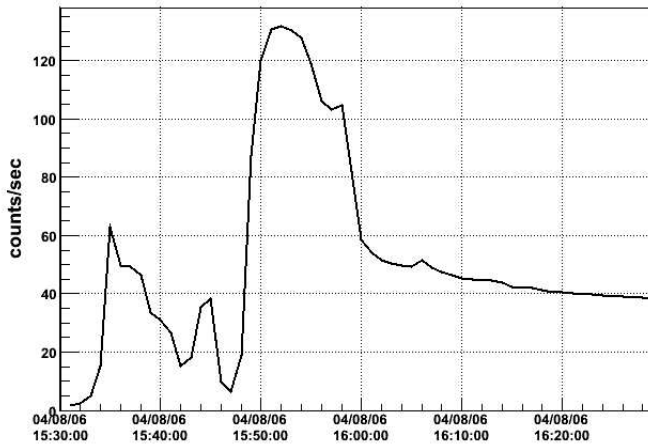


Fig. 14.

the ratio $R_{radii} = 2$ as seen in Figure 17, 18 implying that we probably do have an r^2 dependence in the radiation that the chipmunks receive, in the absence of any magnetic field.

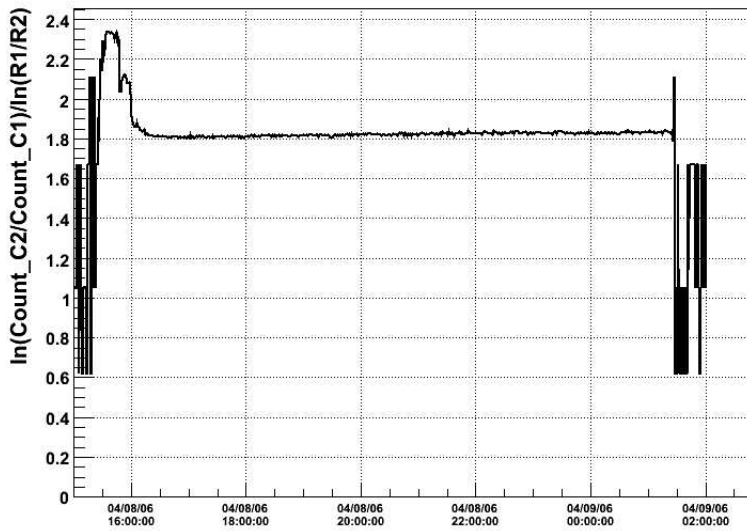


Fig. 15.

For the pre-collimation phase the r dependence is faster than $1/r^2$ but slower than $1/r^3$ as seen in figure 15 and 17 (average $1/r^{2.35}$)

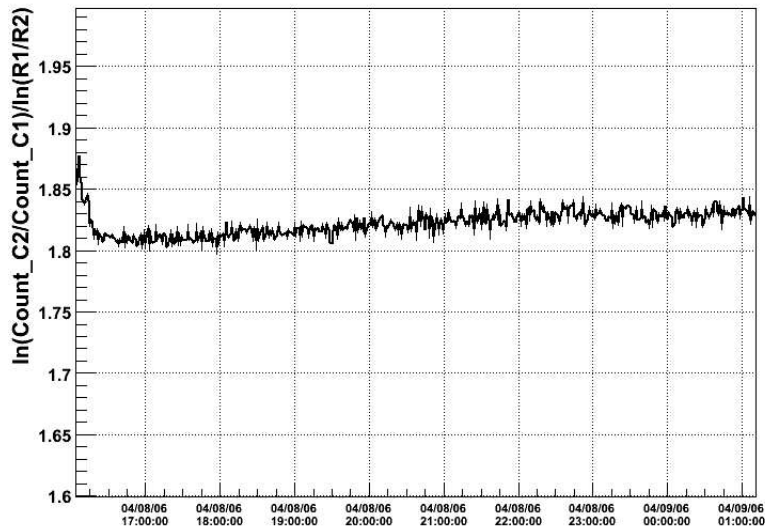


Fig. 16.

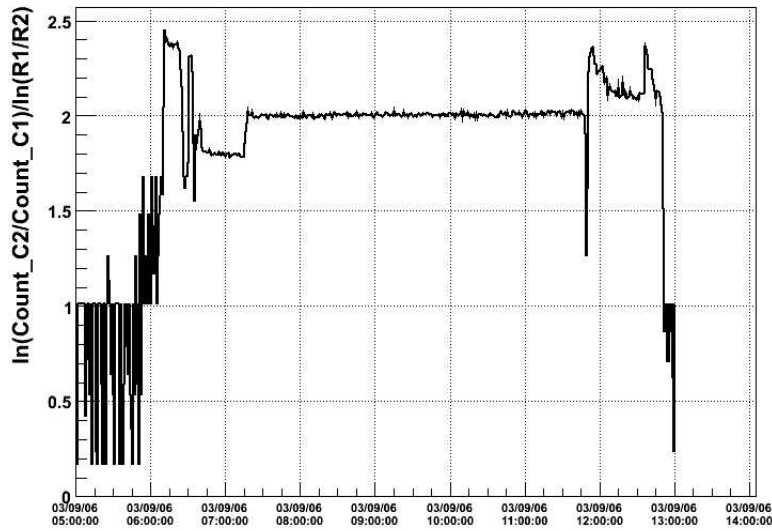


Fig. 17.

5.1.2. *Scaling of Dose with Luminosity*

In order to estimate the radiation dose during RHICII we should examine the dependence of the dose to the delivered luminosities. If the radiation post-collimation is primarily due to collisions then we can extrapolate the currently received dose to RHICII according to the expected luminosities. Thus we examine whether the dose scales with

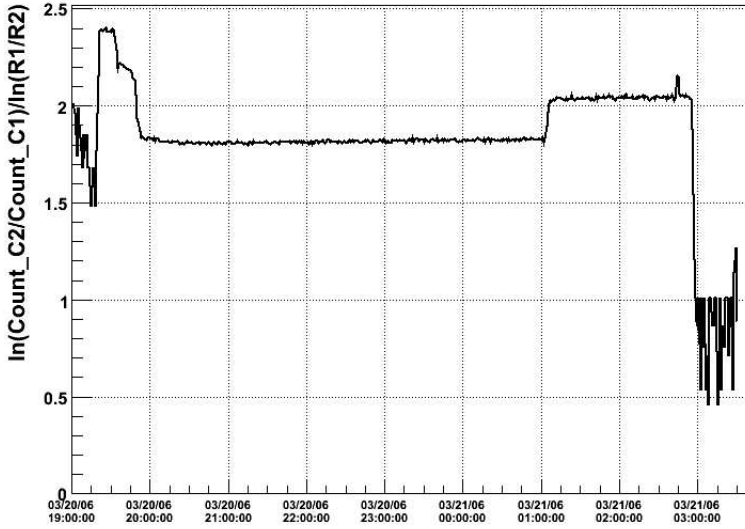


Fig. 18.

luminosity by measuring the Dose/Luminosity variation from store to store. The Luminosity is calculated by using the BBC LL1 trigger count after correcting for the efficiency of the trigger. In figure 19 we see that the Dose/Luminosity ratio (D/L) in $mRad/mb^{-1}$ for chipmunk2, for a number of typical stores which indicate that the Dose scales with Luminosity after collimation. The ratio D/L is almost constant across all stores (with the Luminosity increasing almost by a factor of two) and is $D/L = 0.0015 \cdot 0.000075 mRad/mb^{-1} = 1.5000.075Rad/pb^{-1}$ at 33 cm.

It is important to confirm that the post-collimation dose we observed during run6 operations is actually due to collisions and not scraping, beam-beam interaction or secondary collisions. Thus the C-AD personnel uncogged the beams and the chipmunk dose measurements were obtained for standard beam conditions but without collisions. In the figure 20 we have the ZDC rate on top and the chipmunk count rates on the bottom (in black is the rate of chipmunk1 and in red chipmunk2). We see from the details in figure ?? that during the uncogged phase (where ZDC count =0), chipmunk2 still sees 20% of the dose it sees during collisions and the chipmunk1 sees 14%.

We can estimate the total post collimation dose that was received during the current run by using the observed $D/L = 1.5Rad/pb^{-1}$. The total delivered Luminosity while the Radiation measurement structure was in the IR, is $12pb^{-1}$ and therefore the total estimated post collimation dose is 18Rad. The total dose (pre collimation, post collimation and aborted stores) that the chipmunk2 measured at 33cm was 29.6Rad. The observed average pre-collimation dose is 0.08Rad/store but the variation factor for the pre-collimation dose was bigger than a factor of two. The total received pre-collimation dose was 5 Rad.

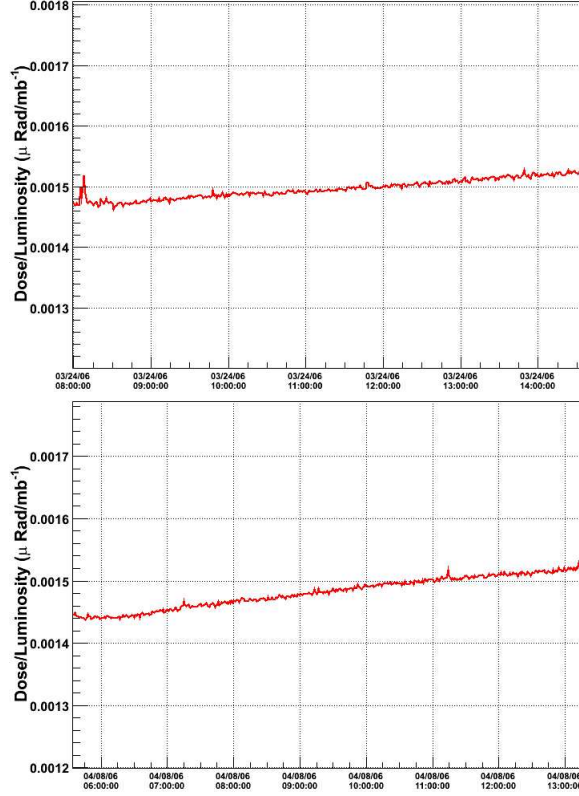


Fig. 19.

5.1.3. Projection to RHICII according to the current PHENIX study

Having established the dependence of the radiation dose on luminosity and radial distance from the Interaction Point, we can extrapolate our current measurements to the RHICII running conditions and estimate the relevant dose expected.

If the measured dose at a state A is DoseA (where A represents the collision species, collision energy, Luminosity, distance from the Interaction Point) then the dose at a different state B would be:

$$Dose_B = Dose_A * \frac{Luminosity_B * Npart_B * c.s._B * (\frac{dN}{dy})_B}{Luminosity_A * Npart_A * c.s._A * (\frac{dN}{dy})_A} \times \left(\frac{R_A}{R_B}\right)^{1.83} \quad (11)$$

Where, Npart is the number of participants, c.s. the p-p cross section and dN/dy the particle yield for p-p at rapidity $y=0$ for the relevant collision energy. We can, therefore, estimate the radiation dose that the strip-pixel sensors will receive after collimation at 10cm, which is the distance of the VTX panels from the I.R., during RHICII operations by using our estimated Dose/Luminosity ratio ($18Rad/12pb^{-1}$) and with the assumption that all the dose will be due to collisions.

For example the expected Luminosity for the 500GeV pp run is $166pb /week$ [1]. If we assume a twenty-week run, the total luminosity delivered during the run would be $3.3fb^{-1}$ thus the expected dose at 10cm, would be $54.61kRad$, according to formula 11. It

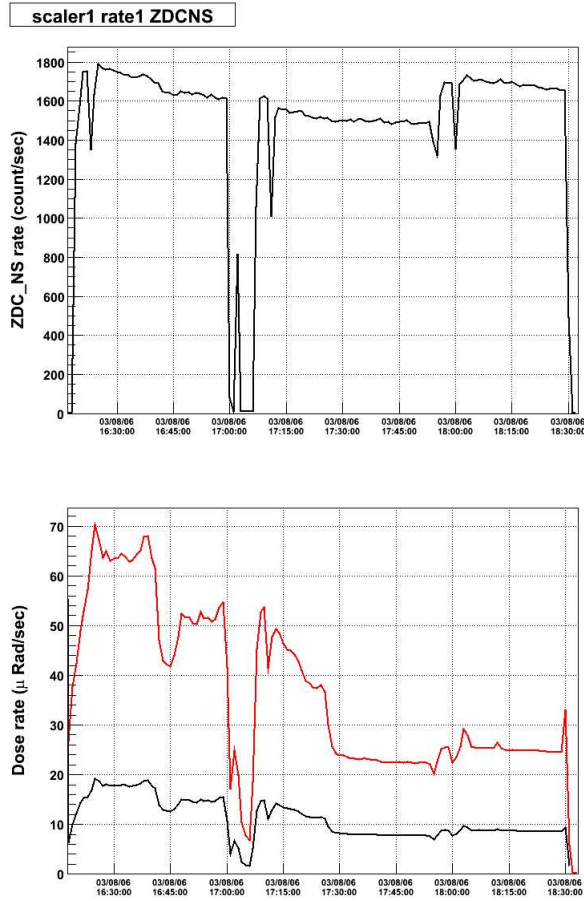


Fig. 20.

is instructive to also express the total dose in equivalent neutron fluence, the conversion factor for which is $1Rad = 1.1810^7 n/cm^2$ [2]. In table 4 there is a summary of the current PHENIX measurement and run conditions and of the expected luminosities [1], cross sections, Nparticipants and estimated radiation doses for a 20 week run for a number of different species and collision energies at RHIC II.

For a ten year run, assuming one year of pp run and nine years of other species (Au-Au, Cu-Cu, pp at 200GeV) the total expected post collimation dose would be $127kRad = 1.510^{12} n/cm^2$.

The pre-collimation phase dependence on beam intensity was studied and the beam quality variations from store to store were such that if any such correlation exists it cannot be observed presently. The average store during the current run has a 0.08 Rad/store radiation dose at 33 cm with a variation factor bigger than two. The scaling with distance is $1/r^{-2.35}$. Assuming a scaling of $1/r^{-2.35}$, 500 stores per year and no dependence on beam intensity the projected dose at 10 cm for a ten year run of RHIC II would be :

$$0.08rad/store \times 10year \times 500stores/year \times (33cm/10cm)^{2.35} = 6.6kRad \quad (12)$$

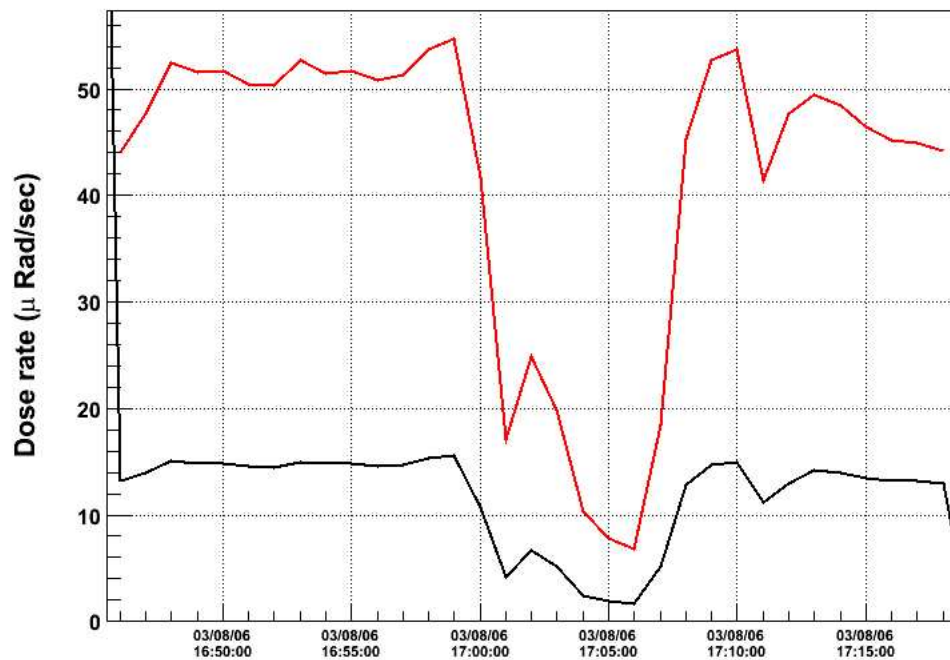


Fig. 21.

Thus the total (pre+post-collimation) expected radiation is $133.6kRad = 1.581012n/cm^2$

Similarly we can repeat these calculations using the total measured dose, which includes the pre-collimation, post collimation phases and aborted stores, at $33\text{ cm} (30Rad/12pb^{-1})$. If we use formula (1) and the total measured radiation dose then the expected radiation for a ten year run at RHICII would be $212kRad = 2.51012n/cm^2$.

Table 4

PHENIX measurement - post collimation								
Species	\sqrt{s} GeV	dN/dy at y=0	Npart	cross section (b)	Radius (cm)	Luminosity (nb^{-1})	Φ_{eq} (n, 1MeV)	Dose (kRad)
pp	200	3.6	2	4.210^{-2}	33	1.210^4	2.1210^8	0.018
Projection at 10cm for 20 week RHIC II runs								
Species	\sqrt{s} GeV	dN/dy at y=0	Npart	cross section (b)	Radius (cm)	Luminosity (nb^{-1})	Φ_{eq} (n, 1MeV)	Dose (kRad)
pp	500	4	2	4.710^{-2}	10	3.310^6	6.4410^{11}	54.61
pp	200	3.6	2	4.210^{-2}	10	7.010^5	1.1010^{11}	9.316
AuAu	200	3.6	100	7.0	10	5.010^1	6.6210^{10}	5.612
CuCu	200	3.6	35	3.4	10	5.010^2	1.1110^{11}	9.427

5.1.4. Projection to RHICII according to CDF measurements

The CDF experiment at the Tevatron Collider at Fermilab has also measured the bulk radiation damage in silicon sensors and the dependence of 1MeV equivalent neutron fluence on the sensor radius from the beam and delivered luminosity [3]. The radiation damage in the SVX and SVX' silicon vertex detectors was measured at 3 cm distance from the I.R. via their leakage currents. Their estimated equivalent 1MeV neutron fluence per fb^{-1} for pp at 1.8 TeV is

$$2.19 + 0.6310^{13}r[cm]^{-1.68}neqcm^{-2}/fb-1 \quad (13)$$

Using formula 11 but with the r-dependence that was observed at CDF ($r^{-1.68}$) we can project their measurement for RHICII conditions. In table 5 there is a summary of the CDF measurement and run conditions and of the expected luminosities [1], cross sections, Nparticipants and estimated radiation doses for a 20 week run for a number of different species and collision energies at RHIC II.

For a ten year run, assuming one year of pp run and nine years of other species (AuAu, CuCu, pp at 200 GeV) the total expected dose according to the CDF measurement would be 248 kRad = 2.98 10¹² n/cm² .

5.2. TLD

The TLDs are used to measure the accumulated radiation during the run (for the duration that the structure was the IR). They are positioned close to the strip-pixels and on the chipmunks and BLMs, as seen in figure 22, so they can be used to cross-check the measurements from the chipmunks and pin-diodes and in order to study in detail the radiation dependence on position. Two TLDs were placed on each of the chipmunks and BLMs (ten TLDs total). A set of 12 TLDs were placed on the strip that was placed 10 cm underneath and run parallel to the beam line, as shown in figure 22. The center axis of the strip was offset by 2 cm from the beam line. Finally six TLDs were positioned on the nose cone (three on the north side and three on the south) at radii where the vertex detector electronics will be positioned (5.08cm, 10.16cm, 15.24cm).

Table 5

CDF measurement									
Species	\sqrt{s} GeV	dN/dy at y=0	Npart	cross section (b)	Radius (cm)	Luminosity (nb^{-1})	Φ_{eq} (n, 1MeV)	$\delta\Phi_{eq}$ (n, 1MeV)	Dose (kRad)
pp	1800	4.3	2	5.210^{-2}	3	1.010^6	3.4710^{12}	6.9510^{11}	289.5
Projection at 10cm for 20 week RHIC II runs									
Species	\sqrt{s} GeV	dN/dy at y=0	Npart	cross section (b)	Radius (cm)	Luminosity (nb^{-1})	Φ_{eq} (n, 1MeV)	Dose (kRad)	
pp	500	4	2	4.710^{-2}	10	3.310^6	1.2810^{12}	5.1010^{11}	106.3
pp	200	3.6	2	4.210^{-2}	10	7.010^5	2.1810^{11}	8.7010^{10}	18.1
AuAu	200	3.6	100	7.0	10	5.010^1	1.3010^{11}	5.1810^{10}	10.8
CuCu	200	3.6	35	3.4	10	5.010^2	2.2010^{11}	8.8110^{10}	18.3

TLD positions in the IR

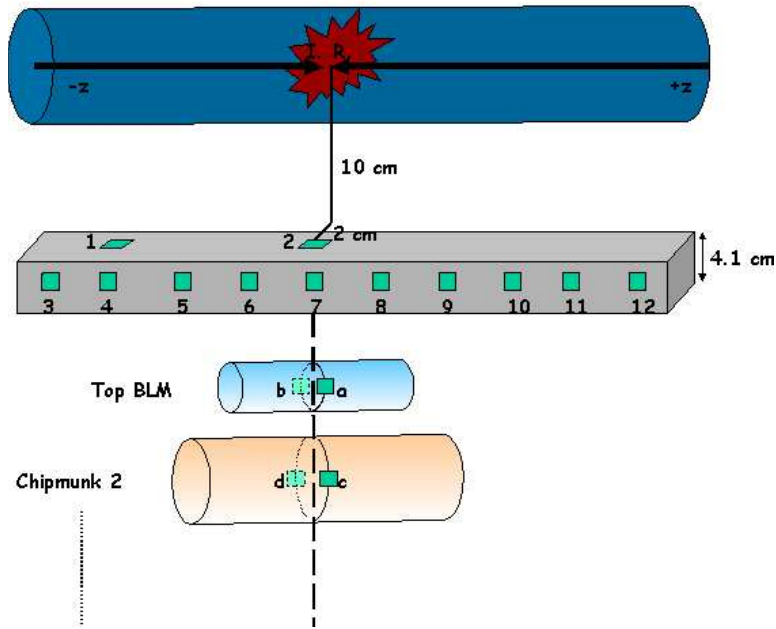


Fig. 22.

5.2.1. TLD measurements Dependence on radial distance from the Interaction Point

The readings from all the TLDs placed at the same z position as the Interaction Point ($z=0$) can be used to obtain the radial dependence of the radiation from the Interaction Point (IP). Two TLDs were placed on each of the chipmunks and BLMs but one of the TLDs that were attached to the last BLM (78.6 cm from IP) came off when the structure was being installed so there is only one measurement for that position. The readings from those TLDs together with the readings from TLD 2 and 7 that were located on the strip parallel to the beam line at $z=0$ are used to study the radial dependence of the radiation. On Table 3 we summarize their readings and radial distance (R) from the IP. Note that the pairs of TLDs attached at the same BLM or chipmunk have different R positions. In figure 23 the TLD radiation measurements are plotted versus their distance R from the Interaction Point and fit to the function $p_0 * R^{p_1}$. The estimated R dependence from the fit is $-1.788 + 0.047$, which is in agreement with the R dependence estimated by using just the chipmunk measurement (-1.83).

There is a difference between the values obtained by the TLDs and the chipmunks. Namely chipmunk2 measured a total dose of 29.6 Rad whereas the TLDs attached to it (c, d) measured an average of 20.6 Rad. Also chipmunk 1 measured a dose of 8.34 Rad whereas the average of the TLDs (g, h) that were attached to it is 4.945 Rad. The reason could be that the TLDs sensitivity to neutrons is 7%. Furthermore the normalization process for obtaining the chipmunk values could be different from the one for the TLDs.

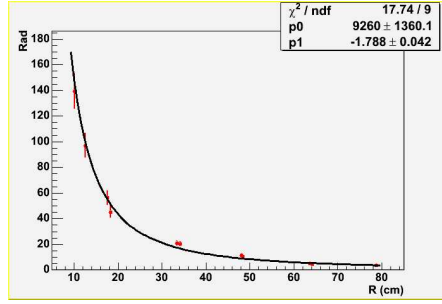


Fig. 23.

5.2.2. TLD measurements - Dependence on distance from the Interaction Point along the beam line

The set of twelve TLDs placed on the strip that run parallel to the beam line (z axis) are used to study the dependence of radiation on z position. TLD 1,2 were placed beside the strip-pixels on the top of the strip, TLD 3-12 were placed on the side of the unistrut, as seen in figure 22. The twelve TLD positions along beam axis, their total radial distance from the IP and the total radiation measured are summarized in table 4 (the $z=0$ position corresponds to the z position of the IP). TLD 1 and TLD 4 have different accumulated values of radiation although they were at the same z -position. Similarly for TLD 2 and TLD 7. However the difference can be accounted for if we take into account the difference in their R positions from the interaction point. TLD 2 is positioned at $R = 10.2$ cm from the IR whereas TLD 7 at $R' = 12.73$ cm from the IP. If we use the R dependence as estimated ($1/R^{1.79}$) then

For TLD 2 :

$$C2 * R^{1.79} = (139.27 * 10.2^{1.79})Rad * cm^{1.79} = (8897.2 + 889.7)Rad * cm^{1.79} \quad (14)$$

For TLD 7:

$$C7 * R'^{1.79} = (97.02 * 12.73^{1.79})Rad * cm^{1.79} = (9215.2 + 921.5)Rad * cm^{1.79}. \quad (15)$$

TLD 2 and TLD 7 measurements are compatible within their 10% accuracy. Same for TLD 1 and TLD 4.

In figure 24 the TLD 3-12 measured doses have been plotted with respect to their z -positions. In order to better examine the z -dependence of the radiation we plot the dose measurements scaled by ($1/R^{1.79}$) with respect to the z position as seen in figure 25. We observe a clear z -dependence, after accounting for the radial dependence, namely the radiation increases as we go closer to the nose cone, which is probably the effect of secondary radiation and scattering from the magnet material.

Finally six TLDs were placed on the magnet nose cones which are at 41 cm (south) and 41 cm (north) along the beam line (z -axis). The measured radiation, their radial distance from the beam line are recorded on table 5. A, B, C TLDs were placed on the north pole, D, E, F on the south. TLD F was destroyed while taking it off the magnet pole thus there is no measurement. These TLDs were left in the Interaction Region for the duration of the run (total luminosity $42pb^{-1}$) as opposed to the TLDs on the strip and the ones attached at the BLMs and chipmunks that were in the area only for part of the run with a delivered luminosity of $12pb^{-1}$). Therefore the accumulated radiation values for these TLDs are higher.

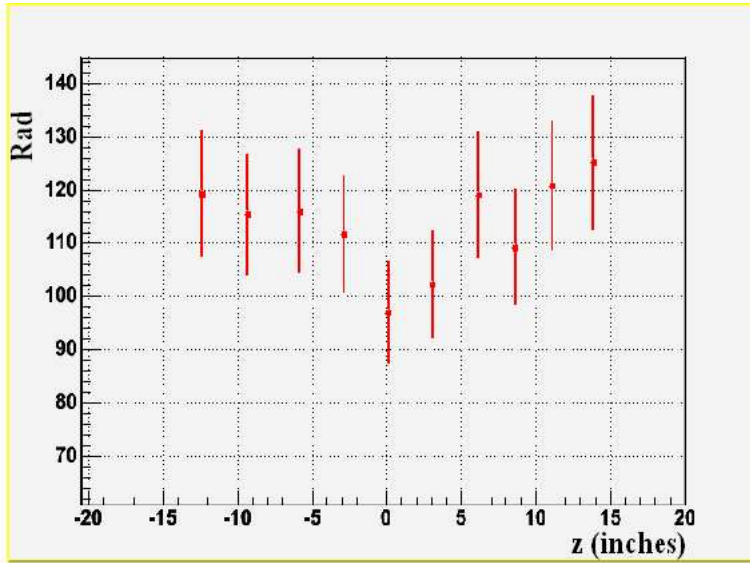


Fig. 24.

In figure ?? the TLD radiation measurements are plotted versus their distance y from the beam pipe and fit to the function $p_0 * R^{p^1}$. The estimated y dependence from the fit is $-1.71 + 0.012$. NOTE THIS IS NOT THE R DISTANCE FROM THE IP BUT THE DISTANCE FROM THE BEAM LINE (Y).

Table 6
TLD 1-12 position along the z-axis, their total radial distance from the IP and the total radiation received

TLD number	z-distance (cm)	R-distance (cm)	Total received radiation (Rad)
1	-24.13	26.20	149.68
2	0	10.2	139.27
3	-31.75	34.21	119.27
4	-24.13	27.28	115.39
5	-15.24	19.86	116
6	-7.62	14.84	111.72
7	0	12.73	97.02
8	7.87	14.97	102.27
9	15.24	19.86	119.06
10	21.59	25.06	109.27
11	27.94	30.7	120.9
12	35.3	37.53	125.19

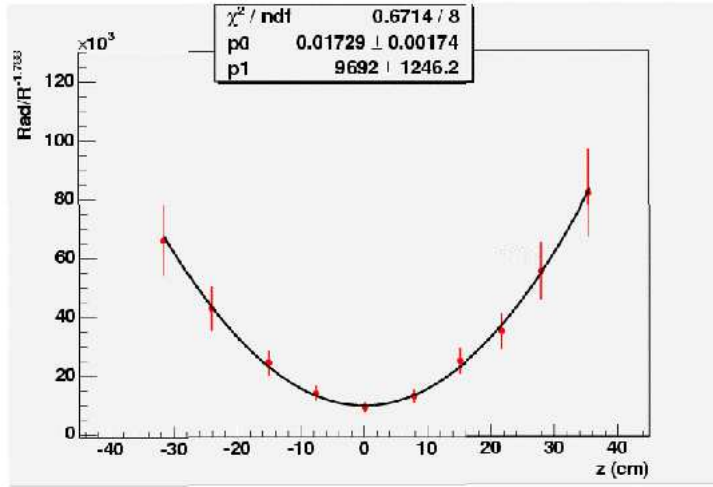


Fig. 25.

5.3. Stripixel Irradiation

The silicon stripixel sensor and 16 monitor diodes set at 10 cm from away beam pipe in PHENIX IR in RUN6. The sensors were irradiated in RUN6 about 50 days. The integrated luminosity was 12 [pb⁻¹].

The damage constant α was estimated 3.2×10^{-17} [A/cm] with the temperature history of thermochlone in PHENIX IR.

The increase of leakage current of single strip was 2.2×10^{-10} [A/strip]. The fluence of irradiated stripixel sensor was estimated to 9.2×10^9 [N_eq/cm²]. The integrated luminosity for 10 years is expected 4000 [pb⁻¹] from 2009. Then the fluence is expected 3.3×10^{12} [N_eq/cm²]. The fluences are summarized in Table. 8. The average fluence of diodes was 1.0×10^{10} [N_eq/cm²]. The fluences were consistent between diodes and stripixel sensor. The estimated z dependence in Fig. 27 is in agreement with it of TLD measurement in Fig. 25.

Table 7

TLD 1-12 position along the z-axis, their total radial distance from the IP and the total radiation received

TLD number	Y distance from IP (cm)	R-distance from IP (cm)	Total received radiation (Rad)±10%
A	5.08	41.31	939.83
B	10.16	42.24	308.88
C	15.24	43.74	158.86
D	5.08	41.31	1052.11
E	10.16	42.24	318.68
F	15.24	43.74	

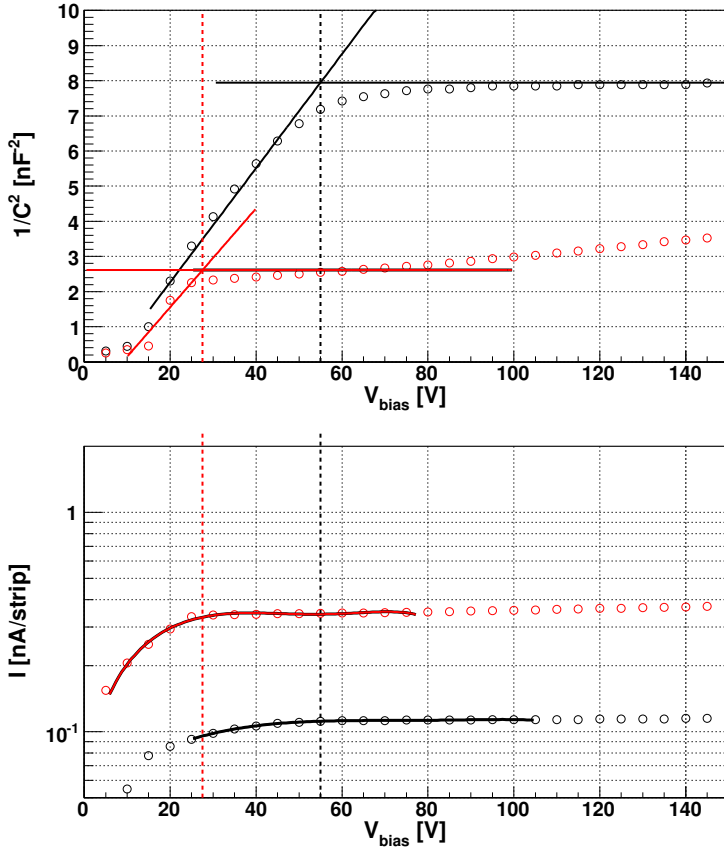


Fig. 26. IV/CV measurements result by stripixel sensor in PHENIX IR

6. Beam irradiation test by stripixel sensor

We studied the fluence dependence of the stripixel sensors irradiated in actual PHENIX environment and beam tests. The setup of 14.1 MeV neutron beam test at Rikkyo Univ. is shown in Fig. 28 and The setup of 16 MeV proton beam test at Univ. of Tsukuba is shown Fig.29. The fluence of proton beam was aiming at the RHIC operation for 10 years; 3×10^{11} [$N_e q/cm^2$]. We studied the increase of leakage current from radiation damage by irradiated with several particles.

6.1. Setup

The fluence of stripixel sensor was estimated by reference diodes. The stripixel sensor was wire-bonded on PCB board for electric measurement, the PCB has 27 Lemo connectors; Bias voltage line, guard ring line, sub-total strip (1512 strips), and isolated 24 single strip line. Then we could measure total current and single strip current before irradiation and after annealing. The annealing temperature was 60 °C for 80 minutes. The increase

of leakage current was estimated at normalized 20 °C. The damage parameter constant α was determined by temperature history of thermoclene which was installed in the same setup.

6.2. Fluence determination

The stripixel sensor and monitor diode were irradiated with 14.1 MeV neutron beam from the Cockcroft-Walton accelerator at Rikkyo. The increase of leakage current of single strip was 3.6×10^{-9} [A/strip]. The fluence of diode at sensor position was estimated 1.3×10^{11} [$N_e q/cm^2$]. The fluence of neutron counter was xxx.

The half of stripixel sensor and monitor diode was irradiated with 16 MeV proton beam from the Tandem accelerator at Tsukuba. The stripixel sensor consists of two half independent sensors. The 20 MeV proton beam was spread by Al board of 0.5 mm thickness, and the beam spread with 16 MeV. The increase of leakage current of single strip was 7.39×10^{-8} [A/strip]. The fluence of diode at sensor position was estimated 2.43×10^{12} [$N_e q/cm^2$].

And there were Cu foil and faraday cup for beam monitor. The fluence of faraday cup was xxx. We evaluated ratio of average intensity of the stripixel sensor and silicon diode to intensity of beam center. Fig. 30 shows intensity distribution of the proton beam. The ratio of average intensity of the stripixel sensor to intensity of beam center is about 93%. The ratio of average intensity of the silicon diode to intensity of beam center is about 73%

Table 8
Fluence of irradiated stripixel sensor and diodes at R=10 cm in PHENIX IR

	Z-distance (cm)	$\Delta I/V$ [A/cm ³]	Error $\Delta I/V$ [A/cm ³]	Fluence [$N_e q/cm^2$]	Error Fluence [$N_e q/cm^2$]
stripixel sensor	25.2	3.0×10^{-7}	2.5×10^{-8}	9.4×10^9	8.6×10^8
diode 1	33.5	4.5×10^{-7}	5.6×10^{-8}	1.4×10^{10}	2.8×10^9
diode 2	33.5	3.1×10^{-7}	5.7×10^{-8}	9.7×10^9	2.0×10^9
diode 3	16.8	2.1×10^{-7}	6.8×10^{-8}	6.7×10^{19}	2.2×10^9
diode 4	16.8	4.7×10^{-7}	5.4×10^{-8}	1.5×10^{10}	2.9×10^9
diode 5	8.9	2.5×10^{-7}	8.1×10^{-8}	7.7×10^9	2.6×10^9
diode 6	8.9	2.8×10^{-7}	7.6×10^{-8}	8.7×10^9	2.5×10^9
diode 7	-7.1	2.1×10^{-7}	7.5×10^{-8}	6.4×10^9	2.4×10^9
diode 8	-7.1	2.5×10^{-7}	4.9×10^{-8}	7.7×10^9	1.4×10^9
diode 9	-13.7	2.3×10^{-7}	1.2×10^{-7}	7.0×10^9	3.9×10^9
diode 10	-13.7	3.1×10^{-7}	5.6×10^{-8}	9.5×10^9	1.9×10^9
diode 11	-20.3	3.5×10^{-7}	1.3×10^{-7}	1.1×10^{10}	4.0×10^9
diode 12	-20.3	2.6×10^{-7}	8.1×10^{-8}	8.0×10^9	2.6×10^9
diode 13	-26.9	3.6×10^{-7}	7.4×10^{-8}	1.1×10^{10}	2.4×10^9
diode 14	-26.9	4.1×10^{-7}	6.9×10^{-8}	1.3×10^{10}	2.3×10^9
diode 15	-33.5	5.3×10^{-7}	5.3×10^{-8}	1.7×10^{10}	3.2×10^9

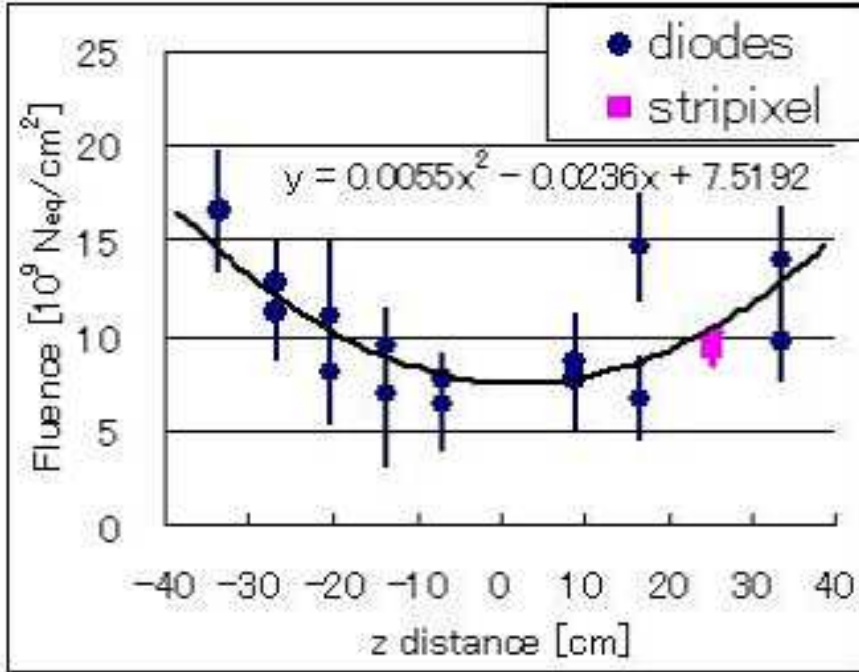


Fig. 27. Fluence of irradiated stripixel sensor and diodes at R=10 cm in PHENIX IR

Table 9
Beam test result with stripixel sensors

stripixel sensor	1	2
Beam particle	neutron	proton
Beam energy [MeV]	14.1	16
$\Delta I/V$ [A/cm ³]	4.76×10^{-6}	9.86×10^{-5}
α [A/cm]	4.04×10^{-17}	4.30×10^{-17}
stripixel sensor fluence [N_{eq}/cm^2]	1.18×10^{11}	2.29×10^{10}
Reference diode fluene [N_{eq}/cm^2]	1.37×10^{11}	$2.xx \times 10^{10}$

6.3. Leakage current of stripixel sensor

We measured two irradiated stripixel sensors with 1.3×10^{11} , 2.43×10^{12} [N_{eq}/cm^2] with 14.1 MeV neutron beam and 16 MeV proton beam, respectively. The increase of leakage current was xxx and xxx, respectively.

It was consistent between neutron beam result and proton beam result on Eq. 1 in Fig. X.

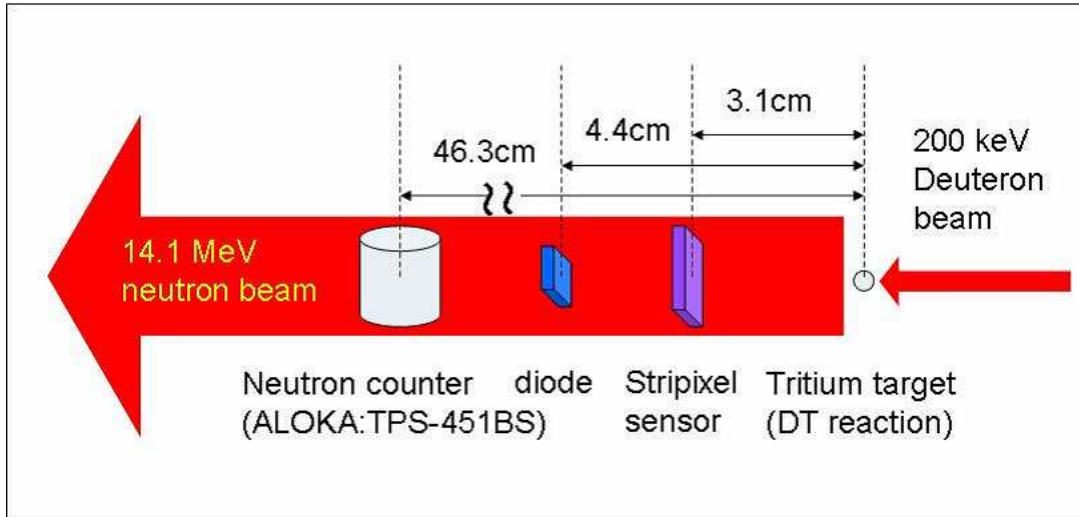


Fig. 28. Beam test setup with 12 MeV proton

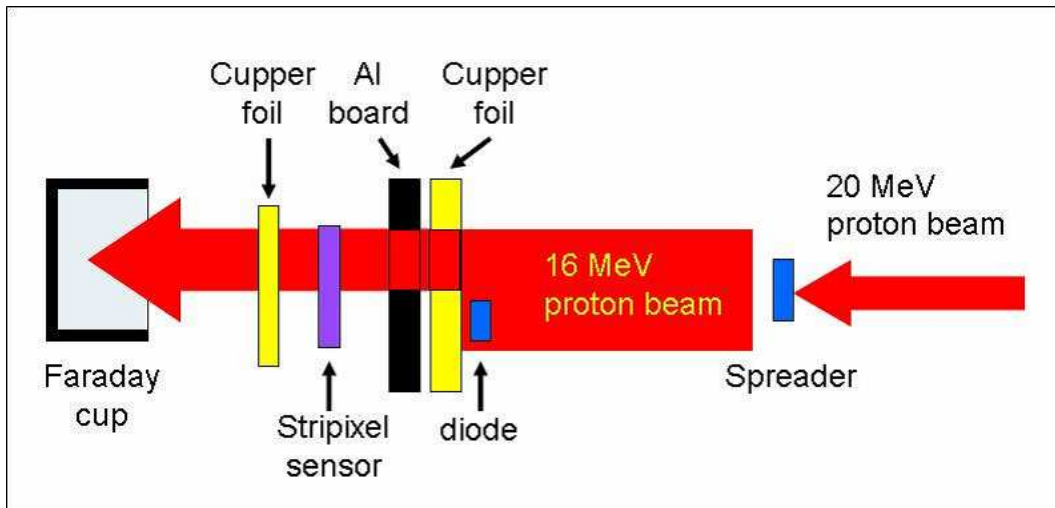


Fig. 29. Beam test setup with 14.1 MeV neutron

6.4. Temperature dependence

We measured the temperature dependence of leakage current with irradiated stripixel sensor. A leakage current I [A] depends on the temperature T [K] as:

$$I = AT^2 \exp(-E_g/2k_B T) \quad (16)$$

Here, A is the sensor constant; E_g is the energy gap of silicon ($E_g = 1.2 \text{ eV}$); and k_B is the Boltzmann constant ($k_B = 8.6 \times 10^{-5} \text{ eV/K}$).

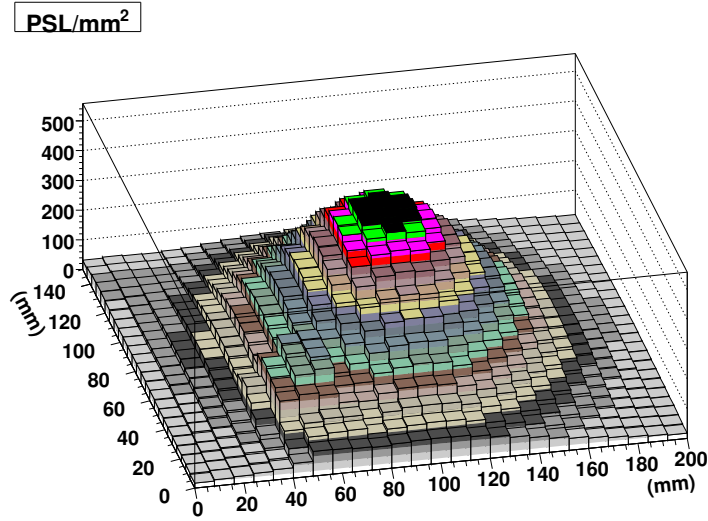


Fig. 30. intensity distribution of proton beam. Unit of PSL is proportional to the number of ^{63}Zn .

7. IUCF irradiation test

8. Results and Conclusion

asai-san will write. The silicon stripixel detector will be installed for vertex tracker in PHENIX from 2009. We studied the radiation damage of stripixel sensor. The silicon diodes were used fluence monitor. The behavior of irradiation stripixel sensor consists of the expectations show as a function of the radiation damage. The fluence expected $3.3\text{E}+12$ [neq/cm²] for 10 years operation from 2009. It is necessary to operate by 0degree or less for the problem of the saturation of front end electronics.

And the increase of leakage current of single strip was 2.2×10^{-10} [A/strip] in PHENIX IR.

The three results measured at 20 °C are on the same line $\Delta I/V = \alpha \Phi_{eq}$ in Fig. ???. Then such color lines are estimated in Fig. ???. The saturation of circuit at 15 nA/strip crosses the expected fluence $\Phi_{eq} = 3.1 \times 10^{12}$ Neq/cm² for RHIC2 running around 0 °C line. Then the required operating temperature of stripixel sensor needs to be about 0 °C to avoid current saturation due to radiation damage.

References

- [1] Z. Li, et al., Nucl. Instr.and Meth. A 518 (2004) 300-304
- [2] Z. Li, et al., Nucl. Instr.and Meth. A 535 (2004) 404-409
- [3] B. Krieger et al.: IEEE Trans. Nucl. Sci. **51** 1968 (2004).

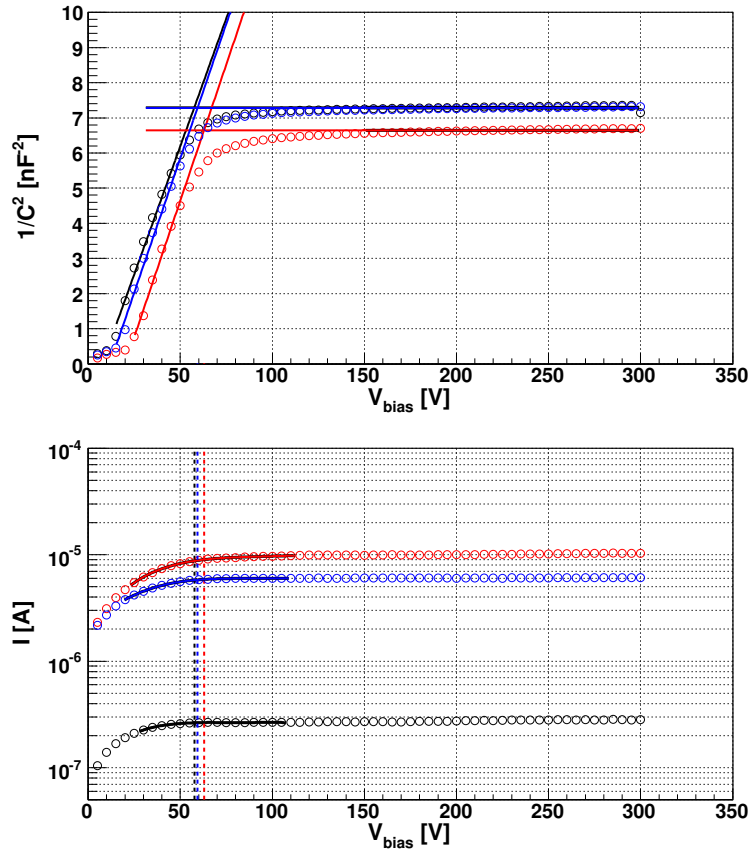


Fig. 31. IV/CV measurements result by stripixel sensor with 14.1 MeV neutron beam

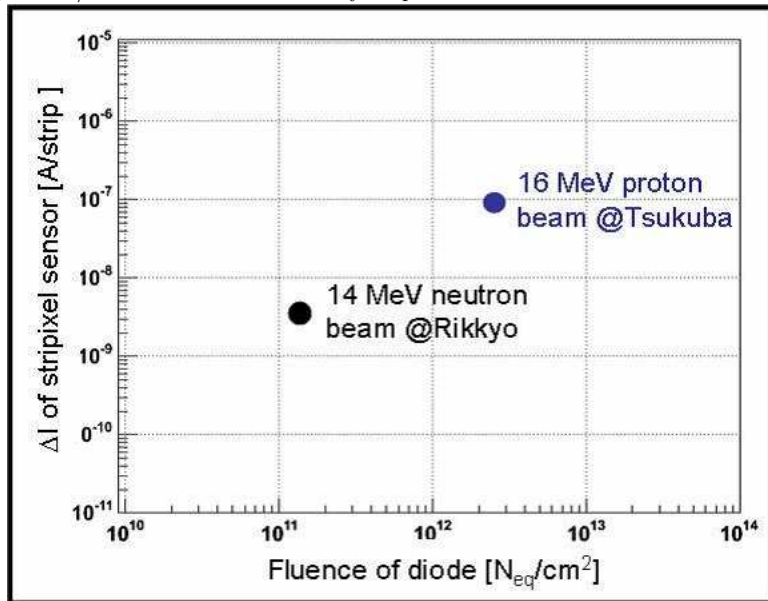


Fig. 32. Distribution of comparison fluence between diode and beam information